

Electronic Supplementary Information (ESI)

**A self-organized sandwich structure of chromium nitride for
ultra-long lifetime in liquid sodium**

Ming Lou ^a, Ran Chen ^a, Kai Xu ^a, Jibin Pu ^{a,*}, Keke Chang ^{a,b,*}

^a *Key Laboratory of Advanced Marine Materials, Ningbo Institute of Materials Technology and Engineering, Chinese Academy of Sciences, Ningbo 315201, China*

^b *Center of Materials Science and Optoelectronics Engineering, University of Chinese Academy of Sciences, Beijing 100049, China*

* Corresponding authors. pujibin@nimte.ac.cn; changkeke@nimte.ac.cn

Methods

1. Coating preparation

The coatings were deposited via multi-arc ion plating using an industrial Hauzer Flexicoat 850 system equipped with one Cr target (purity 99.99 wt%). Si (100) wafers and 316L stainless steels (30 mm × 20 mm × 2 mm, mirror-polished) were used as substrates for microstructure analyses and property measurements. The base pressure of the chamber was less than 4×10^{-3} Pa, the temperature of the substrate holder was 400 °C, and the rotation speed was 3 rad/min. The coating was deposited in an argon gas atmosphere (pressure: 3 Pa) via the following steps: (1) the ion sputter cleaning was performed through substrate biasing at -900, -1100, and -1200 V for 3 min; (2) the Cr transition layer was prepared for 10 min; (3) the CrN coating was deposited in the presence of nitrogen gas under a constant chamber pressure of 3 Pa and deposition time of 12 h. During deposition, a target current of 60 A and a substrate bias of -20 V were applied to the Cr target.

2. Sample characterization

To mimic the service condition of materials in sodium-cooled fast reactors (SFRs), we prepared a tightly sealed container filled with sodium. The CrN-coated 316L SS samples were annealed at 500 °C in the liquid sodium for 1000, 3000, and 6000 h. The composition and structure of the coatings were characterized via scanning electron microscopy (Thermo Scientific Verios G4 UC, U.S.) coupled with energy dispersive X-ray spectroscopy (EDS), X-ray diffraction (XRD, Bruker D8 ADVANCE DAVINCI, Germany), electron backscatter diffraction (EBSD, Oxford Symmetry, U.K.), and transmission electron microscopy (TEM, Thermo Scientific Talos F200x, U.S.); while the cross-sectional specimens were prepared via the focused ion beam technique (Carl Zeiss Auriga, Germany). The mechanical properties, including the nano-hardness and the elastic modulus of the coatings, were determined using a nano-indenter (MTS Nano Indenter G200, U.S.) with a Berkovich diamond tip. The tribological behavior of the coatings was evaluated through ball-on-disc reciprocating sliding tests (CETR UMT-3, U.S.) against tungsten carbide counterfaces in an air atmosphere at 25 °C. The coefficient of friction (COF) data

were continuously recorded during the sliding tests performed for 1 h under a constant load of 1 N, a reciprocating stroke of 5 mm, and a reciprocating frequency of 5 Hz.

3. Phase diagram calculation

The phase diagrams were calculated using the CALPHAD approach, which is based on the basic theory of thermodynamics. This approach was applied to establish a thermodynamic model to describe the Gibbs energy of each constituent phase (gas, liquid, solid solution, and compound) in the material system. The thermodynamic parameters were optimized using data derived from experiments, first-principles calculations, statistical analyses, and semi-empirical analyses¹. The thermodynamic parameters of the Cr-N, Cr-Fe-N, and Cr-Na-N systems were adapted from Ref.²⁻⁴. The phase diagrams at a total pressure of 1 bar were computed using the established dataset and the Thermo-Calc software. The Cr-N phase diagram was computed over a temperature range of 0~1800 °C. The Cr-Fe-N and Cr-Na-N isothermal sections at 500 °C (the immersion test temperature) were calculated.

4. AIMD simulation

Ab initio molecular dynamics (AIMD) simulations based on the density functional theory⁵ were performed for the CrN/Cr, CrN/Na, and Cr₂N/Na interfaces, using the Vienna *ab initio* Simulation Package (VASP)^{6,7}. The projector augmented-wave and the generalized gradient approximation methods were applied in all calculations⁸, and the total energy was calculated using Blöchl corrections⁹. The time step was 1.0 fs, and each simulation task lasted for 10000 fs. The simulation box of Cr/CrN contained 112 atoms, of which 32 body-centered-cubic (bcc) Cr atoms were placed on the face-centered-cubic (fcc) CrN supercell with five atomic layers. Here, bcc (001) and fcc (001) coherent interfaces were adopted. To build the simulation boxes of CrN/Na (120 atoms) and Cr₂N/Na (112 atoms), we held a configuration of 40 Na atoms at 773 K (canonical ensemble) for 1500 fs. The configuration was then quenched to 0 K at an infinite cooling rate. The obtained Na configuration was located on the fcc CrN (001) and hexagonal-closed packed (hcp) Cr₂N (0001) surfaces. For all three boxes, a vacuum space of 20 Å was introduced to avoid interactions between periodic boundary images. For the simulations, we considered a single point for sampling the Brillouin zone, a plane wave cut-off energy of 520 eV, and spin

polarization. In the AIMD simulations, a temperature of 773 K was controlled in the canonical ensemble (NVT)¹⁰ using the Nosé–Hoover thermostat, according to the experimental work. In addition to the AIMD simulations, we computed the elastic constants of fcc CrN and hcp Cr₂N through the strain-stress method using the VASP software. The elastic moduli of bulk (B) and shear (G) were obtained through the Voigt-Reuss-Hill approach¹¹. Hardness (H_v) was evaluated using the following equation¹²:

$$H_v = 2(k^2 G)^{0.585} - 3$$

where k (*i.e.*, the Pugh's modulus ratio) is equal to G/B .

Supplementary Figures

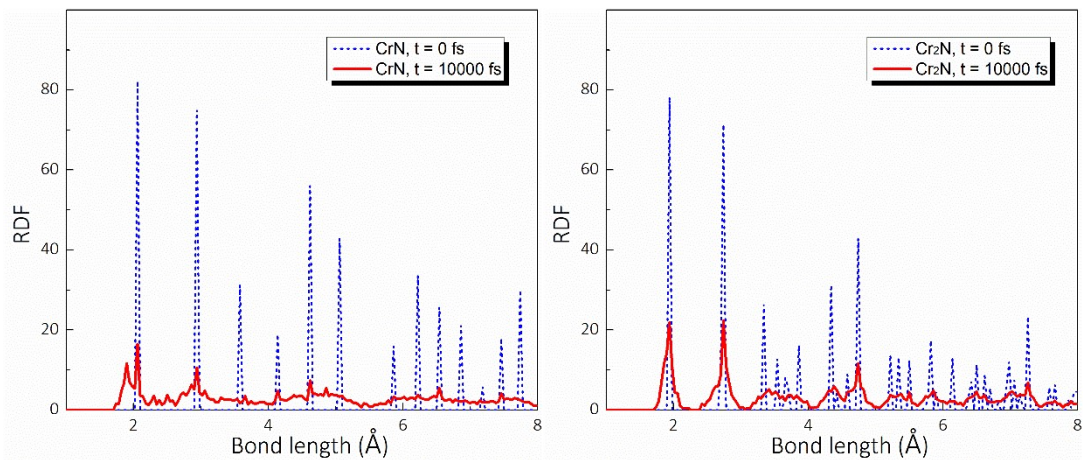
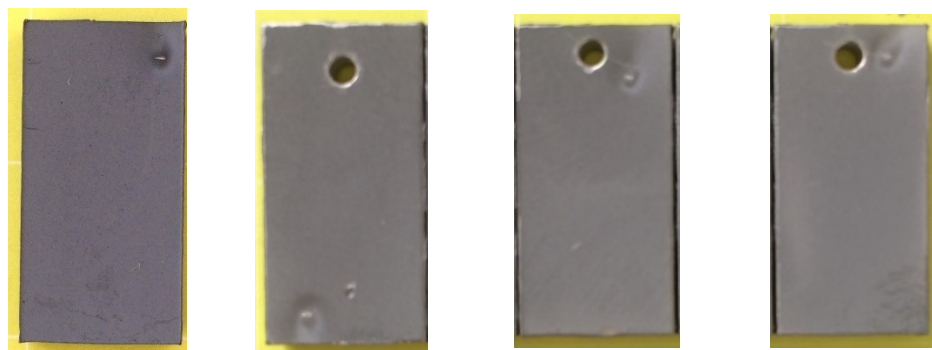


Fig. S1 Average radial distribution functions (RDFs) for the CrN (left) and Cr₂N (right) structures before ($t = 0$ fs) and after ($t = 10000$ fs) the AIMD simulations at 500 °C.



0 h (as-deposited)

1000 h

3000 h

6000 h

Fig. S2 Appearances of the CrN coating after the exposure in liquid sodium at 500 °C for 1000 h, 3000 h, and 6000 h, compared with the as-deposited counterpart. A sheet of notepaper with yellow color was used as the background.

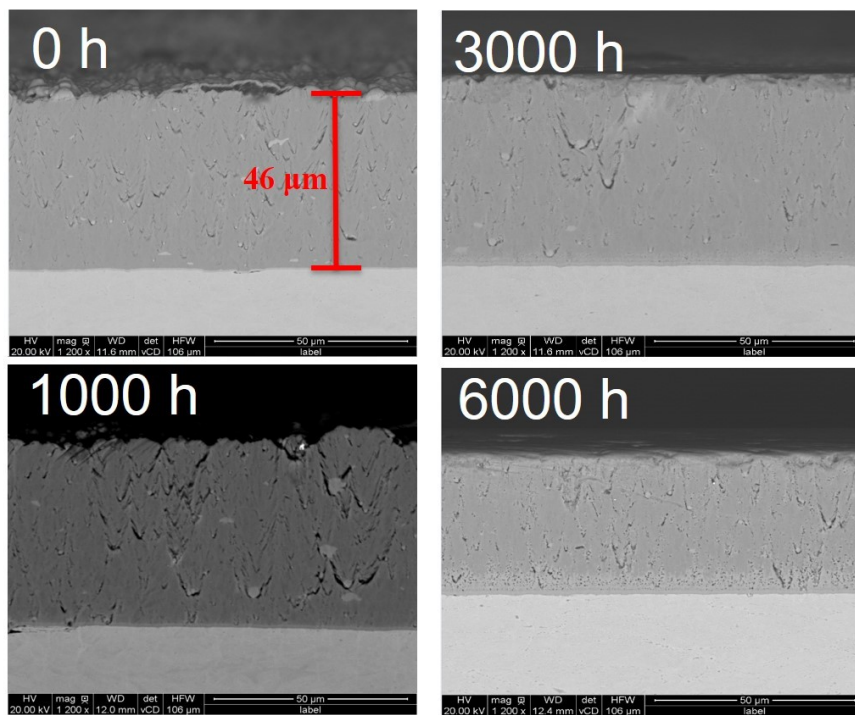


Fig. S3 Backscattered electron (BSE) images of the cross-sections of CrN coatings after the exposure in liquid sodium at 500 °C for 1000 h, 3000 h, and 6000 h, together with the as-deposited counterpart.

Supplementary Data

Cr-Fe-Na-N thermodynamic database

```
$-----
$ Database for Cr-Fe, Cr-Fe, Cr-Na, Cr-N, Fe-N, Na-N, Cr-Fe-N and Cr-Na-N systems
$-----
ELEMENT /- ELECTRON_GAS      0.0000E+00 0.0000E+00 0.0000E+00!
ELEMENT VA VACUUM            0.0000E+00 0.0000E+00 0.0000E+00!
ELEMENT CR BCC_A2            5.1996E+01 4.0500E+03 2.3560E+01!
ELEMENT FE BCC_A2            5.5847E+01 4.4890E+03 2.7280E+01!
ELEMENT N 1/2_MOLE_N2(GAS)   1.4007E+01 4.3350E+03 9.5751E+01!
ELEMENT NA BCC_A2            2.2990E+01 6.4475E+03 5.1447E+01!

SPECIES N2      N2!
SPECIES CR2     CR2!
SPECIES NA2     NA2!
$-----
$ PHASE DEFINITION
$
PHASE LIQUID % 1 1.0 !
CONSTITUENT LIQUID :CR,FE,N,NA : !
$
PHASE BCC_A2 %& 2 1 3 !
CONSTITUENT BCC_A2 :CR,FE,NA : N,VA : !
$
PHASE FCC_A1 %( 2 1 1 !
CONSTITUENT FCC_A1 :CR,FE,NA : N,VA : !
$
PHASE HCP_A3 %) 2 1 .5 !
CONSTITUENT HCP_A3 :CR,FE,NA : N,VA : !
$
PHASE GAS:G % 1 1.0 !
CONSTITUENT GAS:G : CR,CR2,N2,NA,NA2 : !
$
PHASE FE4N % 2 4 1 !
CONSTITUENT FE4N : FE : N : !
PHASE SIGMA % 3 8 4 18 !
CONSTITUENT SIGMA : FE : CR : CR,FE : !
$-----
$ DEFAULTS
TYPE_DEFINITION % SEQ *!
DEFINE_SYSTEM_DEFAULT ELEMENT 2 !
DEFAULT_COMMAND DEF_SYS_ELEMENT VA /- !
TYPE_DEFINITION ( GES A_P_D FCC_A1 MAGNETIC -3.0 2.80000E-01 !
TYPE_DEFINITION ) GES A_P_D HCP_A3 MAGNETIC -3.0 2.80000E-01 !
TYPE_DEFINITION & GES A_P_D BCC_A2 MAGNETIC -1.0 4.00000E-01 !
$
$ ELEMENT DATA from SGTE substance database, Thermo-calc Company, Sweden, 2008.
$
$ CR
FUNCTION GLIQCRCR 298 +GHSERCR+24339.955-11.420225*T+2.37615E-21*T**7; 2180 Y
-16459.984+335.616316*T-50*T*LN(T); 6000 N !
```


FUNCTION GFCCCR 298 +GHSERCR+7284+.163*T; 6000 N !
 FUNCTION GHSERCR 298 -8856.94+157.48*T-26.908*T*LN(T)+.00189435*T**2
 -1.47721E-06*T**3+139250*T**(-1); 2180 Y
 -34869.344+344.18*T-50*T*LN(T)-2.88526E+32*T**(-9); 6000 N !
 FUNCTION GHCPGR 298 +GHSERCR+4438; 6000 N !
 FUNCTION F7491T 2.98150E+02 +390765.331-31.5192158*T-21.36083*T*LN(T)
 +7.253215E-04*T**2-1.588679E-07*T**3+10285.15*T**(-1); 1.10000E+03 Y
 +393886.928-44.1074654*T-19.96003*T*LN(T)+.001513089*T**2
 -4.23648333E-07*T**3-722515*T**(-1); 2.00000E+03 Y
 +421372.003-231.888524*T+5.362886*T*LN(T)-.00848877*T**2
 +2.984635E-07*T**3-6015405*T**(-1); 3.30000E+03 Y
 +305164.699+251.019831*T-55.20304*T*LN(T)+.005324585*T**2
 -2.850405E-07*T**3+34951485*T**(-1); 5.10000E+03 Y
 +1069921.1-1708.93263*T+175.0508*T*LN(T)-.025574185*T**2
 +4.94447E-07*T**3-4.4276355E+08*T**(-1); 7.60000E+03 Y
 -871952.837+1686.47356*T-204.5589*T*LN(T)+.007475225*T**2
 -4.618745E-08*T**3+1.423504E+09*T**(-1); 1.00000E+04 N !
 FUNCTION F7763T 2.98150E+02 +598511.403+41.5353212*T-40.56798*T*LN(T)
 +.004961847*T**2-1.61216717E-06*T**3+154422.85*T**(-1); 8.00000E+02 Y
 +613345.232-104.207991*T-19.7643*T*LN(T)-.007085085*T**2
 -4.69883E-07*T**3-1738066.5*T**(-1); 1.40000E+03 Y
 +642608.843-369.28626*T+17.64743*T*LN(T)-.02767321*T**2
 +1.605906E-06*T**3-5831655*T**(-1); 2.30000E+03 Y
 +553119.895+159.188555*T-52.07969*T*LN(T)-.004229401*T**2
 +1.5939925E-07*T**3+14793625*T**(-1); 3.90000E+03 Y
 +347492.34+623.137623*T-105.0428*T*LN(T)+3.9699545E-04*T**2
 +1.51783483E-07*T**3+1.4843765E+08*T**(-1); 5.80000E+03 Y
 -484185.055+2598.25559*T-334.7145*T*LN(T)+.028597625*T**2
 -4.97520167E-07*T**3+7.135805E+08*T**(-1); 6000 N !
 PAR G(LIQUID,CR;0) 298 +GLIQCR; 6000 N !
 PAR G(BCC_A2,CR:VA;0) 298 +GHSERCR; 6000 N !
 PAR TC(BCC_A2,CR:VA;0) 298 -311.5; 6000 N !
 PAR BMAGN(BCC_A2,CR:VA;0) 298 -.008; 6000 N !
 PAR G(FCC_A1,CR:VA;0) 298 +GFCCCR; 6000 N !
 PAR TC(FCC_A1,CR:VA;0) 298 -1109; 6000 N !
 PAR BMAGN(FCC_A1,CR:VA;0) 298 -2.46; 6000 N !
 PAR G(HCP_A3,CR:VA;0) 298 +GHCPGR; 6000 N !
 PAR TC(HCP_A3,CR:VA;0) 298 -1109; 6000 N !
 PAR BMAGN(HCP_A3,CR:VA;0) 298 -2.46; 6000 N !
 PAR G(GAS,CR;0) 298 +F7491T+R*T*LN(1E-05*P); 6000 N !
 PAR G(GAS,CR2;0) 298 +F7763T+R*T*LN(1E-05*P); 6000 N !
 \$
 \$ Fe
 \$
 FUNCTION GLIQFE 298 +GHSERFE+12040.17-6.55843*T-3.67516E-21*T**7; 1811 Y
 -10838.83+291.302*T-46*T*LN(T); 6000 N !
 FUNCTION GFCCFE 298 -236.7+132.416*T-24.6643*T*LN(T)-.00375752*T**2
 -5.8927E-08*T**3+77359*T**(-1); 1811 Y
 -27097.3963+300.252559*T-46*T*LN(T)+2.78854E+31*T**(-9); 6000 N !
 FUNCTION GHSERFE 298 +1225.7+124.134*T-23.5143*T*LN(T)-.00439752*T**2
 -5.8927E-08*T**3+77359*T**(-1); 1811 Y
 -25383.581+299.31255*T-46*T*LN(T)+2.29603E+31*T**(-9); 6000 N !
 FUNCTION GHCPFE 298 -2480.08+136.725*T-24.6643*T*LN(T)-.00375752*T**2

-5.8927E-08*T**3+77359*T**(-1); 1811 Y
 -29340.776+304.561559*T-46*T*LN(T)+2.78854E+31*T**(-9); 6000 N !

PAR G(LIQUID,FE;0) 298 +GLIQFE; 6000 N !
 PAR G(BCC_A2,FE:VA;0) 298 +GHSERFE; 6000 N !
 PAR TC(BCC_A2,FE:VA;0) 298 +1043; 6000 N !
 PAR BMAGN(BCC_A2,FE:VA;0) 298 +2.22; 6000 N !
 PAR G(FCC_A1,FE:VA;0) 298 +GFCCFE; 6000 N !
 PAR TC(FCC_A1,FE:VA;0) 298 -201; 6000 N !
 PAR BMAGN(FCC_A1,FE:VA;0) 298 -2.1; 6000 N !
 PAR G(HCP_A3,FE:VA;0) 298 +GHCPFE; 6000 N !

\$
 \$ N

FUNCTION GHSERNN 298 -3750.675-9.45425*T-12.7819*T*LN(T)
 -.00176686*T**2+2.681E-09*T**3-32374*T**(-1); 950 Y
 -7358.85+17.2003*T-16.3699*T*LN(T)-6.5107E-04*T**2+3.0097E-08*T**3
 +563070*T**(-1); 3350 Y
 -16392.8+50.26*T-20.4695*T*LN(T)+2.39754E-04*T**2-8.333E-09*T**3
 +4596375*T**(-1); 6000 N !

FUNCTION GLIQNN 298 +GHSERNN+29950+59.02*T; 6000 N !
 FUNCTION GASN2 298 +2*GHSERNN; 6000 N !
 PAR G(LIQUID,N;0) 298 +GLIQNN; 6000 N !
 PAR G(GAS,N2;0) 298 +2*GHSERNN; 6000 N !

\$
 \$ NA

FUNCTION GLIQNA 298 +GHSERNA+2581.02-6.95218*T-2.76132E-18*T**7; 370.87 Y
 -8400.44+192.587343*T-38.1198801*T*LN(T)+.009745854*T**2
 -1.70664E-06*T**3+34342*T**(-1); 2300 N !

FUNCTION GFCCNA 298 +GHSERNA-50+1.3*T; 2300 N !
 FUNCTION GHSERNA 298 -11989.434+260.548732*T-51.0393608*T*LN(T)
 +.072306633*T**2-4.3638283E-05*T**3+132154*T**(-1); 370.87 Y
 -11009.884+199.619999*T-38.1198801*T*LN(T)+.009745854*T**2
 -1.70664E-06*T**3+34342*T**(-1)+1.65071E+23*T**(-9); 2300 N !

FUNCTION GHCPNA 298 +GHSERNA+104+2*T; 2300 N !
 FUNCTION F13051T 298 +101202.044-12.9290072*T-21.02539*T*LN(T)
 +1.9194285E-04*T**2-2.37558167E-08*T**3+6714.165*T**(-1); 2.70000E+03 Y
 +123818.458-80.8203219*T-13.00233*T*LN(T)-6.87485E-04*T**2
 -3.3153E-08*T**3-10435685*T**(-1); 5.50000E+03 Y
 +200317.377-314.322311*T+14.94379*T*LN(T)-.0049580625*T**2
 +8.45444167E-08*T**3-45680820*T**(-1); 9.60000E+03 Y
 -248549.945+382.618817*T-61.81729*T*LN(T)+8.73722E-04*T**2
 +1.54938383E-09*T**3+4.4661115E+08*T**(-1); 1.00000E+04 N !

FUNCTION F13092T 298 +131697.685+6.55101008*T-35.05636*T*LN(T)
 -.0039954535*T**2+5.82776667E-07*T**3-20127.66*T**(-1); 8.00000E+02 Y
 +123510.411+75.1001474*T-44.47351*T*LN(T)-5.345085E-04*T**2
 +6.400745E-07*T**3+1150765*T**(-1); 1.50000E+03 Y
 +79657.0273+417.408691*T-91.76357*T*LN(T)+.022097085*T**2
 -1.3875195E-06*T**3+8765605*T**(-1); 3.10000E+03 Y
 +841444.171-2436.16812*T+261.4099*T*LN(T)-.0509968*T**2
 +1.46319E-06*T**3-3.005069E+08*T**(-1); 4.80000E+03 Y
 -471200.866+911.741259*T-131.5149*T*LN(T)+.0011608825*T**2
 +1.68225167E-07*T**3+5.200375E+08*T**(-1); 6000 N !

PAR G(LIQUID,NA;0) 298 +GLIQNA; 2300 N !

PAR G(BCC_A2,NA:VA;0) 298 +GHSERNA; 2300 N !
 PAR G(FCC_A1,NA:VA;0) 298 +GFCCNA; 2300 N !
 PAR G(HCP_A3,NA:VA;0) 298 +GHCPNA; 2300 N !
 PAR G(GAS,NA;0) 298 +F13051T+R*T*LN(1E-05*P); 6000 N !
 PAR G(GAS,NA2;0) 298 +F13092T+R*T*LN(1E-05*P); 6000 N !
 \$-----
 \$ Binary system
 \$-----
 \$
 \$ Cr-N from Frisk1991
 \$ Frisk, K. . "A thermodynamic evaluation of the Cr-N, Fe-N, Mo-N and Cr-Mo-N systems." \$
 Calphad 15.1(1991):79-106.
 \$
 PAR L(LIQUID,CR,N;0) 298 -161800-16.11*T; 6000 N !
 PAR L(LIQUID,CR,N;1) 298 65508; 6000 N !
 PAR G(BCC_A2,CR:N;0) 298 GHSERCR+1.5*GASN2+311870+29.12*T; 6000 N !
 PAR L(BCC_A2,CR:N,VA;0) 298 -200000; 6000 N !
 PAR TC(BCC_A2,CR:N,VA;0) 298 -311.5; 6000 N !
 PAR BMAGN(BCC_A2,CR:N,VA;0) 298 -0.008; 6000 N !
 PAR G(FCC_A1,CR:N;0) 298 GHSERCR+0.5*GASN2-124460+142.16*T-8.5*T*LN(T);
 6000 N !
 PAR L(FCC_A1,CR:N,VA;0) 298 20000; 6000 N !
 PAR TC(FCC_A1,CR:N,VA;0) 298 -1109; 6000 N !
 PAR BMAGN(FCC_A1,CR:N,VA;0) 298 -2.46; 6000 N !
 PAR G(HCP_A3,CR:N;0) 298 GHSERCR+0.25*GASN2-65760+64.69*T-3.93*T*LN(T);
 6000 N !
 PAR L(HCP_A3,CR:N,VA;0) 298 21120-10.61*T; 6000 N !
 PAR L(HCP_A3,CR:N,VA;1) 298 -6204; 6000 N !
 \$-----
 \$
 \$ Cr-Na from Hao2012
 \$ Hao, D., et al. "Thermodynamic modeling of the Na-X (X = Si, Ag, Cu, Cr) systems."
 \$ Journal of Mining and Metallurgy Section B Metallurgy 48.2(2012):273-282.
 \$
 PAR L(LIQUID,CR,NA;0) 298 56433; 6000 N !
 PAR L(BCC_A2,CR,NA:VA;0) 298 49609; 6000 N !
 PAR L(HCP_A3,CR,NA:VA;0) 298 8E4; 6000 N !
 PAR L(FCC_A1,CR,NA:VA;0) 298 8E4; 6000 N !
 \$-----
 \$ Fe-Cr from Lee1993
 \$ Lee, Byeong Joo . "A thermodynamic evaluation of the Fe-Cr-Mn-C system."
 \$ Metallurgical Transactions A 24.5(1993):1017-1025.
 \$
 PAR G(LIQUID,CR,FE;0) 298 -17737+7.996546*T; 6000 N !
 PAR G(LIQUID,CR,FE;1) 298 -1331; 6000 N !
 PAR G(BCC_A2,CR,FE:VA;0) 298 20500-9.68*T; 6000 N !
 PAR BMAGN(BCC_A2,CR,FE:VA;0) 298 -.85; 6000 N !
 PAR TC(BCC_A2,CR,FE:VA;0) 298 1650; 6000 N !
 PAR TC(BCC_A2,CR,FE:VA;1) 298 550; 6000 N !
 PAR G(FCC_A1,CR,FE:VA;0) 298 10833-7.477*T; 6000 N !
 PAR G(FCC_A1,CR,FE:VA;1) 298 1410; 6000 N !
 PAR G(HCP_A3,CR,FE:VA;0) 298 10833-7.477*T; 6000 N !
 PAR G(SIGMA,FE:CR:CR;0) 298 +8*GFCCFE+22*GHSERCR+92300-95.96*T; 6000 N !

PAR G(SIGMA,FE:CR:FE;0) 298 +8*GFCCFE+4*GHSERCR+18*GHSERFE+117300-95.96*T;
6000 N !

\$-----

\$

\$ FE-N from Gorbachev2009

\$ Gorbachev, I. I., and V. V. Popov . "Analysis of the solubility of carbides, nitrides, and
\$ carbonitrides in steels using methods of computer thermodynamics: III. Solubility of carbides,
\$ nitrides, and carbonitrides in the Fe-Ti-C, Fe-Ti-N, and Fe-Ti-C-N systems."

\$ Physics of Metals & Metallography 108.5(2009):484-495.

\$

PAR L(LIQUID,FE,N;0) 298 -19930-12.01*T; 6000 N !

PAR G(BCC_A2,FE:N;0) 298 93562+165.07*T+GHSERFE+3*GHSERNN; 6000 N !

PAR TC(BCC_A2,FE:N;0) 298 1043; 6000 N !

PAR BMAGN(BCC_A2,FE:N;0) 298 2.22; 6000 N !

PAR G(FCC_A1,FE:N;0) 298 -37460+375.42*T-37.6*T*LN(T)+GHSERFE+GHSERNN;
6000 N !

PAR L(FCC_A1,FE:VA,N;0) 298 -26150; 6000 N !

PAR TC(FCC_A1,FE:N;0) 298 -201; 6000 N !

PAR BMAGN(FCC_A1,FE:N;0) 298 -2.1; 6000 N !

PAR G(HCP_A3,FE:N;0) 298 -12015+37.98*T+GHSERFE+0.5*GHSERNN; 6000 N !

PAR L(HCP_A3,FE:VA,N;0) 298 +10345-19.71*T; 6000 N !

PAR L(HCP_A3,FE:VA,N;1) 298 -11130+11.84*T; 6000 N !

PAR G(Fe4N,FE:N;0) 298 -38744+73.52*T+4*GHSERFE+GHSERNN; 6000 N !

\$-----

Supplementary References

1. Z.-K. Liu, *Acta Mater.*, 2020, **200**, 745-792.
2. D. Hao, M. Bu, Y. Wang, Y. Tang, Q. Gao, M. Wang, B. Hu, Y. Du, *J. Min. Metall. B*, 2012, **48**, 273-282.
3. K. Frisk, *Calphad*, 1991, **15**, 79-106.
4. I. I. Gorbachev, V. V. Popov, *Phys. Met. Metall.*, 2009, **108**, 484.
5. P. Hohenberg, W. Kohn, *Phys. Rev.*, 1964, **136**, B864-B871.
6. G. Kresse, J. Hafner, *Phys. Rev. B*, 1993, **48**, 13115-13118.
7. G. Kresse, J. Hafner, *Phys. Rev. B*, 1994, **49**, 14251-14269.
8. G. Kresse, D. Joubert, *Phys. Rev. B*, 1999, **59**, 1758-1775.
9. P. E. Blöchl, *Phys. Rev. B*, 1994, **50**, 17953-17979.
10. N. Shuichi, *Prog. Theor. Phys. Supp.*, 1991, **103**, 1-46.
11. G. Simmons, H. Wang, *Single crystal elastic constants and calculated aggregate properties: A handbook*, M.I.T Press, Cambridge, 1971.
12. X.-Q. Chen, H. Niu, D. Li, Y. Li, *Intermetallics*, 2011, **19**, 1275-1281.